

# A New Approach to the Control of a Hydraulic Stewart Platform

M. R. Sirouspour and S. E. Salcudean  
University of British Columbia  
Vancouver, BC, Canada  
shahins@ece.ubc.ca, tims@ece.ubc.ca

**Abstract:** Novel stable adaptive nonlinear controllers are proposed for position tracking control of hydraulic manipulators. The controllers were developed by using the backstepping approach and are based on realistic models that include rigid body dynamics, friction, and hydraulic actuator dynamics with valve orifice and spool displacement nonlinearities. Using Lyapunov analysis, it is shown that tracking errors are bounded and converge to zero in the absence of Coulomb friction and are bounded when Coulomb friction is present. The proposed techniques were used to control a hydraulic Stewart platform. Their effectiveness were confirmed by simulations and experiments.

## 1. Introduction

Hydraulic robots and machinery are widely used in the construction and mining industries, as well as in motion simulators. They have rapid responses and high power-to-weight ratios which suit these applications. Currently, linear controllers, e.g. P.D., are commonly used to control hydraulic robots, since they are simple to implement. Their level of performance is limited because of the highly nonlinear nature of the hydraulic actuator dynamics.

The high performance control of robot manipulators has been the subject of much research. Examples include computed torque techniques [1], passivity based techniques [2], adaptive control techniques [3], and robust control methods [4]. Provably stable controllers that account for rigid body and actuator dynamics have been developed for electrically-driven robots (e.g., [5]), but the authors are aware of only two reports of provably stable hydraulic robot controllers that account for both actuator and rigid body dynamics [6, 7]. While the problem of single cylinder hydraulic control has been studied analytically and experimentally [8, 9], other work in hydraulic robot control (e.g., [10] using singular perturbations, [11] using decentralized adaptive control, and [12] using pressure feedback control) does not include complete stability proofs and contains limited experimental and simulation results.

This paper addresses the high performance control of a hydraulic Stewart platform. Following the authors' earlier work in [9, 7], novel nonlinear position tracking controllers are proposed for hydraulic robots using *backstepping*. The controllers are augmented with adaptation laws to compensate for parametric uncertainties in the system dynamics. In order to avoid acceleration feed-

back, the first controller is augmented with a passivity-based adaptive observer while the second one features a robust sliding type observer. The adaptive controller/adaptive observer is proven to be semi-globally asymptotically stable. The asymptotic stability of the adaptive controller/sliding observer is also shown via Lyapunov analysis. In the presence of friction in the actuators, it can be shown that the tracking errors become bounded.

These approaches are different from the method proposed in [6] mainly in the form of the observers and the way they are coupled with the controllers. This is especially evident in the case of the second controller that features a robust observer. The proposed controllers were implemented to control a hydraulic Stewart platform. The simulation and experimental results demonstrate excellent position tracking performance for these new methods.

Following this section, a short description of the system model is given in Section 2. The control approaches are described in Section 3. Section 4 presents the simulation results. Section 5 discusses implementation issues and experimental results. Conclusions are drawn in Section 6.

## 2. Rigid Body/Actuators Dynamics

The dynamic model of a robot manipulator driven by single-rod hydraulic actuators is composed of two parts, namely rigid body and hydraulics dynamics. The dynamics of  $n$ -link rigid body robots are governed by a second order nonlinear differential equation

$$D(q)\ddot{q} + C(q, \dot{q})\dot{q} + G(q) = \tau, \quad (1)$$

where  $q \in R^n$  is the generalized joint position vector and  $\tau \in R^n$  is the generalized joint torque vector.  $D(q) \in R^{n \times n}$  is the manipulator mass matrix,  $C(q, \dot{q}) \in R^{n \times n}$  a matrix containing coriolis and centrifugal terms and  $G(q) \in R^n$  is a vector representing the gravitational effects. Equation (1) can also be rewritten in a *linear-in-parameters* form which is convenient for the application of adaptive control techniques:

$$D(q)\ddot{q} + C(q, \dot{q})\dot{q} + G(q) = Y(q, \dot{q}, \ddot{q})\theta, \quad (2)$$

where  $Y(q, \dot{q}, \ddot{q})$  is a regressor matrix and  $\theta \in R^m$  is the vector of unknown rigid body parameters. The rigid body dynamics of the UBC motion simulator, the experimental setup, are given in *Appendix B*. The leg dynamics have been ignored in deriving this model. It is possible to include these dynamics in the system model, however, the resultant model would become very complex and only little improvement may be achieved. Unlike electrically driven manipulators, hydraulic robots exhibit significant nonlinear actuator dynamics. These dynamics can be expressed in the following form (assuming a three-way valve configuration)

$$\dot{\tau} = f(q, \dot{q}) + g(q, \tau, u), \quad (3)$$

where  $u \in R^n$  is the control command vector and  $f, g \in R^n$  are nonlinear functions of  $q, \dot{q}$  and  $\tau$ . The expressions for  $f$  and  $g$  are given in *Appendix A*.

This equation can also be described in the linear-in-parameters format

$$\dot{\tau} = f_0(q, \dot{q})\gamma_1 + g_0(q, \tau, u)\gamma_2, \quad (4)$$

where  $\gamma_1 = [\gamma_1^1 \ \dots \ \gamma_1^n]^T$ ,  $\gamma_2 = [\gamma_2^1 \ \dots \ \gamma_2^n]^T$  are two sets of hydraulic parameters as defined in *Appendix A* and  $f_0, g_0$  are defined by:

$$f_0(q, \dot{q}) = \text{diag}\{f_0^i(q^i, \dot{q}^i)\}, \quad g_0(q, \tau, u) = \text{diag}\{g_0^i(q^i, \tau^i, u^i)\} \quad (5)$$

This model addresses the nonlinearities in spool displacement and valve orifice.

Note that (1) describes the rigid body dynamics in joint-space coordinates. An alternative approach is to represent these dynamics in task-space coordinates. All of the arguments made in this paper are applicable to task-space coordinates with only minor changes in the derivation.

### 3. Control Approach

The system to be controlled is a third-order nonlinear system subject to parametric uncertainties both in rigid body and hydraulic dynamics. In this section two methods are proposed for the control of this system. The following Lemma [13] will be used in the stability proof.

*Lemma 1:* Consider the scalar function  $\alpha = (\theta - \hat{\theta})^T(\rho - \hat{\rho})$ , with  $\theta, \hat{\theta}, \rho \in R^n$  and  $a^i \leq \theta^i \leq b^i$ . Then, if  $\hat{\theta} = \kappa(a, b, \rho)\rho$  where  $\kappa(a, b, \rho)$  is a diagonal matrix with entries

$$\kappa^i(a, b, \rho) = \begin{cases} 0 & \text{if } \hat{\theta}^i \leq a^i, \rho^i \leq 0 \\ 0 & \text{if } \hat{\theta}^i \geq b^i, \rho^i \geq 0 \\ 1 & \text{otherwise} \end{cases} \quad (6)$$

it follows that  $\alpha \leq 0$ .

#### 3.1. Adaptive Controller with Adaptive Observer

An adaptive controller is proposed for the control of hydraulic robots modeled by (1) and (3). An adaptive observer is also presented to avoid using acceleration feedback in the control law. Throughout this section, the following notation will be used:

$$\begin{aligned} \dot{q}_r &= \dot{q}_d - \Lambda_1(\hat{q} - q_d) = \dot{q}_d - \Lambda_1(e - \tilde{q}) & \dot{q}_o &= \dot{\hat{q}} - \Lambda_2(q - \hat{q}) = \dot{\hat{q}} - \Lambda_2\tilde{q} \\ s_1 &= \dot{q} - \dot{q}_r = \dot{e} + \Lambda_1(e - \tilde{q}) & s_2 &= \dot{q} - \dot{q}_o = \dot{\tilde{q}} + \Lambda_2\tilde{q}, \end{aligned} \quad (7)$$

where  $\hat{q} \in R^n$  is the estimated value of  $q$ ,  $e = q - q_d$ , and  $\tilde{q} = q - \hat{q}$  are position tracking errors and observation errors, respectively. Furthermore,  $\Lambda_1, \Lambda_2 > 0$  are diagonal. Note that in the definitions of  $\dot{q}_r$  and  $\dot{q}_o$ ,  $\dot{q}$  has been replaced by  $\dot{q}_d$  and  $\dot{\hat{q}}$  which eliminates the need for acceleration feedback as it will be seen later.

*Theorem 1:* Consider the system described by (1), (3), the observer dynamics

$$\begin{aligned}\dot{\hat{q}} &= z + \Lambda_2 \tilde{q} \\ \dot{z} &= \hat{D}_2(q)^{-1} [\tau - \hat{C}_2(q, \dot{q}) \dot{q}_o - \hat{G}_2(q) + L_p \tilde{q} + K_d s_1 + K'_d s_2]\end{aligned}\quad (8)$$

and the controller obtained by solving the following simple algebraic equation

$$g_0(q, \tau, u) \hat{\gamma}_2 = \dot{\tau}_d - f_0(q, \dot{q}) \hat{\gamma}_1 - \Gamma_\tau^{-1} s_1 - K_\tau \tilde{\tau} \quad (9)$$

where

$$\begin{aligned}\tau_d &= \hat{D}_1(q) \ddot{q}_r + \hat{C}_1(q, \dot{q}_r) \dot{q}_r + \hat{G}_1(q) - K_d (s_1 - s_2) - K_p e \\ &= Y(q, \dot{q}_r, \ddot{q}_r) \hat{\theta}_1 - K_d (s_1 - s_2) - K_p e\end{aligned}\quad (10)$$

with unknown rigid body parameter adaptation laws

$$\dot{\hat{\theta}}_1 = -\kappa_{\theta_1} \Gamma_1^{-1} Y^T(q, \dot{q}_r, \ddot{q}_r) s_1, \quad \dot{\hat{\theta}}_2 = -\kappa_{\theta_2} \Gamma_2^{-1} Y^T(q, \dot{q}, \ddot{q}_o) s_2 \quad (11)$$

where

$$Y(q, \dot{q}, \dot{q}_o, \ddot{q}_o) \hat{\theta}_2 = \hat{D}_2(q) \ddot{q}_o + \hat{C}_2(q, \dot{q}) \dot{q}_o + \hat{G}_2(q) \quad (12)$$

and with hydraulic parameter adaptation laws

$$\begin{aligned}\dot{\hat{\gamma}}_1 &= \kappa_{\gamma_1} \Gamma_{\gamma_1}^{-1} \Gamma_\tau f_0(q, \dot{q}) \tilde{\tau} \\ \dot{\hat{\gamma}}_2 &= \kappa_{\gamma_2} \Gamma_{\gamma_2}^{-1} \Gamma_\tau \Pi\left(\frac{\tilde{\tau}}{\hat{\gamma}_2}\right) (\dot{\tau}_d - f_0(q, \dot{q}) \hat{\gamma}_1 - \Gamma_\tau^{-1} s_1 - K_\tau \tilde{\tau})\end{aligned}\quad (13)$$

where  $\Pi\left(\frac{\tilde{\tau}}{\hat{\gamma}_2}\right) = \text{diag}\left\{\frac{\tilde{\tau}_i}{\hat{\gamma}_2^i}\right\}$ . Then, if the conditions given below in (14,15) are satisfied,  $\underline{Q}$  is an asymptotically stable equilibrium point of the state  $\tilde{x} = [e^T \quad \tilde{q}^T \quad s_1^T \quad s_2^T \quad \tilde{\tau}^T]^T$ .

$$\begin{aligned}(i) \quad & \underline{\sigma}(K_p) \underline{\sigma}(L_p) \underline{\sigma}(\Lambda_1) \underline{\sigma}(\Lambda_2) > \frac{1}{4} \bar{\sigma}^2(K_p) \bar{\sigma}^2(\Lambda_1) \\ (ii) \quad & \|\tilde{x}(0)\| \leq \sqrt{\frac{\alpha_m}{3\alpha_M} \left( \frac{\underline{\sigma}(K_d) - C_M \dot{q}_{dm}}{C_M \bar{\sigma}(\Lambda_1)} \right)^2 - \frac{V_{p_M} - V_{p_m}}{\alpha_M}}\end{aligned}\quad (14)$$

where

$$\begin{aligned}\alpha_m &= \frac{1}{2} \min\{D_m, \underline{\sigma}(K_p), \underline{\sigma}(L_p), \underline{\sigma}(\Gamma_\tau)\} \\ \alpha_M &= \frac{1}{2} \max\{D_M, \bar{\sigma}(K_p), \bar{\sigma}(L_p), \bar{\sigma}(\Gamma_\tau)\} \\ V_{p_m} &\leq \frac{1}{2} \left( \tilde{\theta}_1^T \Gamma_1 \tilde{\theta}_1 + \tilde{\theta}_2^T \Gamma_2 \tilde{\theta}_2 + \tilde{\gamma}_1^T \Gamma_{\gamma_1} \tilde{\gamma}_1 + \tilde{\gamma}_2^T \Gamma_{\gamma_2} \tilde{\gamma}_2 \right) \leq V_{p_M}\end{aligned}\quad (15)$$

Here,  $\bar{\sigma}(\cdot)$  and  $\underline{\sigma}(\cdot)$  denote the maximum and minimum singular values of their matrix argument, respectively, and  $\dot{q}_{dm}$  is an upper bound on the norm of the

desired velocity. The projection gains  $\kappa_{\theta_1}$ ,  $\kappa_{\theta_2}$ ,  $\kappa_{\gamma_1}$  and  $\kappa_{\gamma_2}$  are defined as in (6).

*Remark:* Condition (ii) in (14) specifies the boundary of the attraction region. Since this boundary can be enlarged arbitrarily, the system is semi-globally asymptotically stable. All the gain matrices are assumed to be diagonal and positive definite. Also note that the controller and the observer are using different sets of estimated parameters. They could also be modified to use the same parameter estimates. The use of projection gains as defined in Lemma 1, guarantees that the estimated parameters remain within predefined levels and therefore the control law is always defined. The proposed control does not require acceleration measurements since there are no velocity terms,  $\dot{q}$ , involved in  $\tau_d$  in (10).

*Proof:* By substituting (10) into (1) the following error dynamics are obtained

$$D(q)\dot{s}_1 + C(q, \dot{q})s_1 + K_d s_1 + K_p e = K_d s_2 - C(q, s_1)(\dot{q} - s_1) - Y(q, \dot{q}_r, \ddot{q}_r)\tilde{\theta}_1 + \tilde{\tau} \quad (16)$$

The observer closed-loop dynamics could also be written as

$$D(q)\dot{s}_2 + C(q, \dot{q})s_2 + K'_d s_2 + L_p \tilde{q} = -K_d s_1 - Y(q, \dot{q}, \dot{q}_o, \ddot{q}_o)\tilde{\theta}_2 \quad (17)$$

where (1) and (8) have been used in deriving (17). Now, let the Lyapunov-like function  $V_1$  be defined as:

$$V_1 = \frac{1}{2}s_1^T D(q)s_1 + \frac{1}{2}e^T K_p e + \frac{1}{2}s_2^T D(q)s_2 + \frac{1}{2}\tilde{q}^T L_p \tilde{q} + \frac{1}{2}\tilde{\theta}_1^T \Gamma_1 \tilde{\theta}_1 + \frac{1}{2}\tilde{\theta}_2^T \Gamma_2 \tilde{\theta}_2 \quad (18)$$

It can be shown that the derivative of  $V_1$  along the trajectory of the closed-loop system is given by

$$\begin{aligned} \dot{V}_1 &\leq -s_1^T K_d s_1 - s_2^T K'_d s_2 - e^T K_p \Lambda_1 e - \tilde{q}^T L_p \Lambda_2 \tilde{q} \\ &\quad + e^T K_p \Lambda_1 \tilde{q} + s_1^T \tilde{\tau} - s_1^T C(q, s_1)(\dot{q}_d - \Lambda_1 e + \Lambda_1 \tilde{q}) \\ &\leq -(\underline{\sigma}(K_d) - C_M(\dot{q}_{dm} + \bar{\sigma}(\Lambda_1)\|e\| + \bar{\sigma}(\Lambda_1)\|\tilde{q}\|))\|s_1\|^2 \\ &\quad - \underline{\sigma}(K'_d)\|s_2\|^2 - \underline{\sigma}(K_p)\underline{\sigma}(\Lambda_1)\|e\|^2 - \underline{\sigma}(L_p)\underline{\sigma}(\Lambda_2)\|\tilde{q}\|^2 \\ &\quad + \bar{\sigma}(K_p)\bar{\sigma}(\Lambda_1)\|e\|\|\tilde{q}\| + s_1^T \tilde{\tau} = H(\|e\|, \|\tilde{q}\|, \|s_1\|, \|s_2\|) + s_1^T \tilde{\tau} \end{aligned} \quad (19)$$

In deriving (19), (16), (17), Lemma 1 and the adaptation laws given in (11) have been used. Note that

$$\begin{aligned} & - \underline{\sigma}(K_p)\underline{\sigma}(\Lambda_1)\|e\|^2 - \underline{\sigma}(L_p)\underline{\sigma}(\Lambda_2)\|\tilde{q}\|^2 + \bar{\sigma}(K_p)\bar{\sigma}(\Lambda_1)\|e\|\|\tilde{q}\| \\ &= - \begin{bmatrix} \|e\| & \|\tilde{q}\| \end{bmatrix} \begin{bmatrix} \underline{\sigma}(K_p)\underline{\sigma}(\Lambda_1) & -\frac{1}{2}\bar{\sigma}(K_p)\bar{\sigma}(\Lambda_1) \\ -\frac{1}{2}\bar{\sigma}(K_p)\bar{\sigma}(\Lambda_1) & \underline{\sigma}(L_p)\underline{\sigma}(\Lambda_2) \end{bmatrix} \begin{bmatrix} \|e\| \\ \|\tilde{q}\| \end{bmatrix} \end{aligned} \quad (20)$$

The condition (i) given in (14) guarantees the positive definiteness of the above matrix. Furthermore, if the following condition is satisfied

$$\|e\| + \|\tilde{q}\| < \frac{\underline{\sigma}(K_d) - C_M \dot{q}_{dm}}{C_M \bar{\sigma}(\Lambda_1)}, \quad (21)$$

then one can write

$$H(\|e\|, \|\tilde{q}\|, \|s_1\|, \|s_2\|) \leq -\alpha(\|e\|^2 + \|\tilde{q}\|^2 + \|s_1\|^2 + \|s_2\|^2) \quad (22)$$

with  $\alpha > 0$ . It is not difficult to show that if (ii) in (14) holds then (21) is also satisfied.

Following the backstepping approach,  $V_2$ , which is a Lyapunov function for the system dynamics, is defined as

$$V_2 = V_1 + \frac{1}{2} \tilde{\tau}^T \Gamma_\tau \tilde{\tau} + \frac{1}{2} \tilde{\gamma}_1^T \Gamma_{\gamma_1} \tilde{\gamma}_1 + \frac{1}{2} \tilde{\gamma}_2^T \Gamma_{\gamma_2} \tilde{\gamma}_2 \quad (23)$$

where  $\tilde{\gamma}_1 = [\tilde{\gamma}_1^1 \ \dots \ \tilde{\gamma}_1^n]^T$  and  $\tilde{\gamma}_2 = [\tilde{\gamma}_2^1 \ \dots \ \tilde{\gamma}_2^n]^T$  are the vectors of hydraulic parameter estimation errors. By taking the derivative of (23) and employing the control law given in (9) and after some manipulation one can show that

$$\begin{aligned} \dot{V}_2 \leq & H(\|e\|, \|\tilde{q}\|, \|s_1\|, \|s_2\|) - \tilde{\tau}^T \Gamma_\tau K_\tau \tilde{\tau} + \tilde{\gamma}_1^T \left[ f_0(q, \dot{q}) \Gamma_\tau \tilde{\tau} - \Gamma_{\gamma_1} \dot{\hat{\gamma}}_1 \right] \\ & + \tilde{\gamma}_2^T \left[ \Gamma_\tau \Pi \left( \frac{\tilde{\tau}}{\tilde{\gamma}_2} \right) (\dot{\tau}_d - f_0(q, \dot{q}) \hat{\gamma}_1 - \Gamma_\tau^{-1} s_1 - K_\tau \tilde{\tau}) - \Gamma_{\gamma_2} \dot{\hat{\gamma}}_2 \right] \end{aligned} \quad (24)$$

Using the adaptation laws given in (13), the derivative of  $V_2$  becomes

$$\dot{V}_2 \leq -\gamma(\|e\|^2 + \|\tilde{q}\|^2 + \|s_1\|^2 + \|s_2\|^2 + \|\tilde{\tau}\|^2) \quad (25)$$

with  $\gamma > 0$ . Therefore the tracking errors converge to zero asymptotically.

*Remark:* The method can be easily modified to use the same set of parameters in the controller and the observer. In this case

$$\dot{\hat{\theta}} = -\kappa_\theta \Gamma^{-1} [Y^T(q, \dot{q}_r, \ddot{q}_r) s_1 + Y^T(q, \dot{q}, \dot{q}_o, \ddot{q}_o) s_2] \quad (26)$$

### 3.2. Adaptive Controller with Sliding Observer

An adaptive controller featuring a sliding-type observer is introduced in this section. By comparison to the previous method, this new approach requires fewer computations. First the following notation is defined:

$$\dot{q}_r = \dot{q}_d - \Lambda e \quad s = \dot{q} - \dot{q}_r = \dot{e} + \Lambda e, \quad (27)$$

where  $e = q - q_d$  and  $q_d, \dot{q}_d, \ddot{q}_d$  are the desired position, velocity and acceleration trajectories, and  $\Lambda > 0$  is a diagonal matrix.

*Theorem 2:* Consider the system described by (1),(3) and the following observer:

$$z = \dot{\hat{q}}, \quad \dot{z} = \Gamma_o \dot{\hat{q}} + \Lambda_o \text{sgn}(\dot{\hat{q}}) - W^T(q, \dot{q}_r, \hat{\theta}) s + \ddot{\hat{q}} \quad (28)$$

with

$$W(q, \dot{q}_r, \hat{\theta}) = -\hat{D}(q)\Lambda + \hat{C}(q, \dot{q}_r) - K_d, \quad \ddot{\tilde{q}} = \bar{D}^{-1} [\tau - \bar{C}\dot{\tilde{q}} - \bar{G}] \quad (29)$$

where  $\bar{D}$ ,  $\bar{C}$  and  $\bar{G}$  are constant matrices and  $\dot{\tilde{q}} = \dot{q} - \hat{q}$  is the velocity observation error. Let the control law be given by the solution  $u$  of the following algebraic equation

$$g_0(q, \tau, u)\hat{\gamma}_2 = \dot{\tau}_d - f_0(q, \dot{q})\hat{\gamma}_1 - \Gamma_\tau^{-1}s - K_\tau\tilde{\tau} \quad (30)$$

with

$$\tau_d = \hat{D}(q)(\ddot{q}_r + \Lambda\dot{\hat{q}}) + \hat{C}(q, \dot{\hat{q}})\dot{q}_r + \hat{G}(q) - K_d(s - \dot{\hat{q}}) - K_p e \quad (31)$$

and let the parameters be adapted according to the following laws

$$\dot{\hat{\theta}} = -\kappa_\theta \Gamma_\theta^{-1} Y^T(q, \dot{q}, \dot{q}_r, \ddot{q}_r) s \quad (32)$$

and

$$\begin{aligned} \dot{\hat{\gamma}}_1 &= \kappa_{\gamma_1} \Gamma_{\gamma_1}^{-1} \Gamma_\tau f_0(q, \dot{q}) \tilde{\tau} \\ \dot{\hat{\gamma}}_2 &= \kappa_{\gamma_2} \Gamma_{\gamma_2}^{-1} \Gamma_\tau \Pi\left(\frac{\tilde{\tau}}{\hat{\gamma}_2}\right) \cdot (\dot{\tau}_d - f_0(q, \dot{q})\hat{\gamma}_1 - \Gamma_\tau^{-1}s - K_\tau\tilde{\tau}) \end{aligned} \quad (33)$$

for the rigid body and hydraulic parameters, respectively, where  $\kappa_\theta$ ,  $\kappa_{\gamma_1}$  and  $\kappa_{\gamma_2}$  are projection gains as defined in (6). Then,  $\underline{Q}$  is an asymptotically stable equilibrium point of the state  $\tilde{x} = \begin{bmatrix} e^T & s^T & \dot{\tilde{q}}^T & \tilde{\tau}^T \end{bmatrix}^T$ .

*Remark :* In Equation (31)

$$\begin{aligned} \ddot{q}_r + \Lambda\dot{\hat{q}} &= \ddot{q}_d - \Lambda(\dot{q} - \dot{q}_d) + \Lambda(\dot{q} - \dot{\hat{q}}) = \ddot{q}_d - \Lambda(\dot{q} - \dot{q}_d) \\ s - \dot{\hat{q}} &= \dot{q} - \dot{q}_r - \dot{q} + \dot{\hat{q}} = \dot{\hat{q}} - \dot{q}_r \end{aligned} \quad (34)$$

Therefore,  $\tau_d$  does not contain any velocity terms. This is a very important point since  $\dot{\tau}_d$  appears in (30) and (33). In other words, the proposed control law does not require acceleration measurements.

*Proof:* By substituting (31) into (1) the following dynamics are obtained

$$D(q)\dot{s} + C(q, \dot{q})s + K_d s + K_p e = -Y(q, \dot{q}, \dot{q}_r, \ddot{q}_r)\tilde{\theta} - W(q, \dot{q}_r, \hat{\theta})\dot{\tilde{q}} + \tilde{\tau} \quad (35)$$

Define the Lyapunov-like function  $V_1$  to be

$$V_1 = \frac{1}{2} e^T K_p e + \frac{1}{2} s^T D(q) s + \frac{1}{2} \dot{\tilde{q}}^T \dot{\tilde{q}} + \frac{1}{2} \tilde{\theta}^T \Gamma_\theta \tilde{\theta} \quad (36)$$

It can be shown that the derivative of  $V_1$  becomes

$$\begin{aligned} \dot{V}_1 &= -s^T K_d s - e^T K_p \Lambda e - \dot{\tilde{q}}^T \Gamma_\theta \dot{\tilde{q}} - \dot{\tilde{q}}^T [\ddot{\tilde{q}} - \ddot{q} + \Lambda_o \text{sgn}(\dot{\tilde{q}})] \\ &\quad + \tilde{\theta}^T [\Gamma_\theta \dot{\tilde{\theta}} - Y^T(q, \dot{q}, \dot{q}_r, \ddot{q}_r) s] + s^T \tilde{\tau}, \end{aligned} \quad (37)$$

where (35) has been used. The adaptation laws in (32) render  $\dot{V}_1$  into

$$\dot{V}_1 = -s^T K_d s - e^T K_p \Lambda e - \dot{\tilde{q}}^T \Gamma_o \dot{\tilde{q}} + \Sigma + s^T \tilde{\tau} \quad (38)$$

where  $\Sigma = -\dot{\tilde{q}}^T [\ddot{\tilde{q}} - \ddot{q} + \Lambda_o \text{sgn}(\dot{\tilde{q}})]$ . It is not difficult to show that

$$\|\ddot{\tilde{q}} - \ddot{q}\| \leq \sigma_0 + \sigma_1 \|\dot{\tilde{q}}\|^2 + \sigma_2 \|\tau\| + \sigma_3 \|\dot{q}\|. \quad (39)$$

Therefore, the following choice for  $\Lambda_o$  renders  $\Sigma < 0$ :

$$\Lambda_o = \text{diag}\{\Lambda_o^i\}, \quad \Lambda_o^i = \lambda_0^i + \lambda_1^i \|\dot{q}\|^2 + \lambda_2^i \|\tau\| + \lambda_3^i \|\dot{q}\| \quad (40)$$

and  $\lambda_k^i > \sigma_k$  for  $i = 1, \dots, n$ ,  $k = 0, \dots, 3$ . The rest of the proof is the same as in *Theorem 1* and will not be presented here. In summary, the controllers proposed in this paper require position, velocity and actuator forces (pressures) to be measured.

### 3.3. Effect of Friction

In the controllers proposed in this paper, friction in the hydraulic actuators has been neglected. It is easy to handle viscous friction since it acts as additional damping in the system. It is also straightforward to show that in the presence of Coulomb friction the tracking errors do not converge to zero but remain bounded. The error bounds can be reduced by increasing the gains. The proof will be omitted here.

## 4. Simulation Results

Simulations have been conducted to investigate the effectiveness of the proposed methods and also to obtain guidelines for performing the experiments. For this purpose the dynamic model of a six-degree-of-freedom hydraulic Stewart platform (see *Appendix B*) and the controller were simulated using the *Matlab Simulink<sup>TM</sup>* toolbox. A task-space control strategy was adopted because of the simpler form of the dynamics in these coordinates. Since in practice the actuator lengths are measured, the forward kinematics must be computed on-line. This was done using Newton's method. The proposed controllers were modified slightly in order to be used in task-space coordinates.

The system parameters were chosen close to those of the experimental setup and are given in Table 1. The controllers performed similarly in simulation and only the results obtained with the adaptive controller/sliding observer are presented here. The tracking errors for a reference trajectory composed of  $x_d = 0.02 \sin(2\pi t) + 0.01 \sin(4\pi t) + 0.01 \sin(6\pi t)$ ,  $y_d = 0$ ,  $z_d = 0.02 \sin(2\pi t) + 0.01 \sin(4\pi t)$ ,  $\psi_d = 0.0873 \sin(2\pi t) + 0.0349 \sin(4\pi t)$ ,  $\theta_d = 0.0524 \sin(2\pi t) + 0.0175 \sin(4\pi t)$ ,  $\phi_d = 0.0524 \sin(2\pi t) + 0.0175 \sin(4\pi t)$  are shown in Figure 1(a). Positions and angles are expressed in meters and radians, respectively. The tracking errors clearly converge to zero. The profiles of the parameter estimates are given in Figure 1(b). The parameter adaption laws were activated after  $t = 0.5 \text{ sec}$ . The parameters converge to their actual values as seen in this figure even though the parameter convergence is not guaranteed in theory.

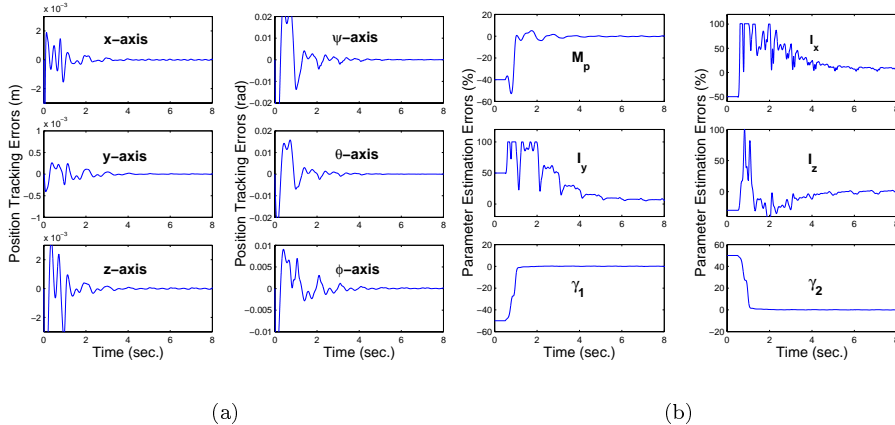


Figure 1. Simulation results. (a) Position tracking errors. (b) Parameter estimation errors.

## 5. Experimental Results

The control methods proposed in this paper were also evaluated experimentally. The University of British Columbia motion simulator (Figure 4) was chosen for this purpose [14]. This simulator uses six 1.5 inch bore, 54 inch stroke hydraulic jacks. The jacks are anchored by roller-bearing U-joints in 120 degree symmetric configurations on the base and platform. Each cylinder is capable of exerting forces in excess of 4000 N at 1 m/s, and over 8000 N at zero rod speed. The hydraulic actuation system is equipped with *Rexroth 4WRDE* three-stage proportional valves connected in a three-way configuration. Low friction Teflon seals are used in the hydraulic cylinders. The installed sensors measure the actuator lengths, the valve spool positions, and the pressures both in the control and supply sides of the cylinders. High bandwidth valves with a bandwidth of around 80Hz have been used in the setup so the dynamics of the valves may be ignored. In order to synthesize the control command an algebraic equation must be solved (Equation (9) or (30)). In practice, the valve spool positions are sensed and employed in the implementation of the controllers. The actuator velocities which are needed in the control law are estimated from the measured actuator lengths using fixed gain Kalman filters. Off-line experiments were performed to identify the initial values of the parameter estimates.

The computational setup was a PC running *VxWorks<sup>TM</sup> 5.4* and a Sparc 1e board running *VxWorks<sup>TM</sup> 5.2* (see Figure 4). The Sparc 1e performs the I/O and safety functions and the controller runs on the PC. The controller was implemented using the *Matlab Real Time Workshop<sup>TM</sup>* toolbox targeting *Tornado<sup>TM</sup> 2.0*. Data between the PC and the VME board are communicated through a custom parallel I/O communication protocol. Using this setup a control frequency of 512 Hz was successfully achieved. The same controller block used in the simulation studies was utilized to control the platform. This is a great advantage of the computational approach adopted in this paper.

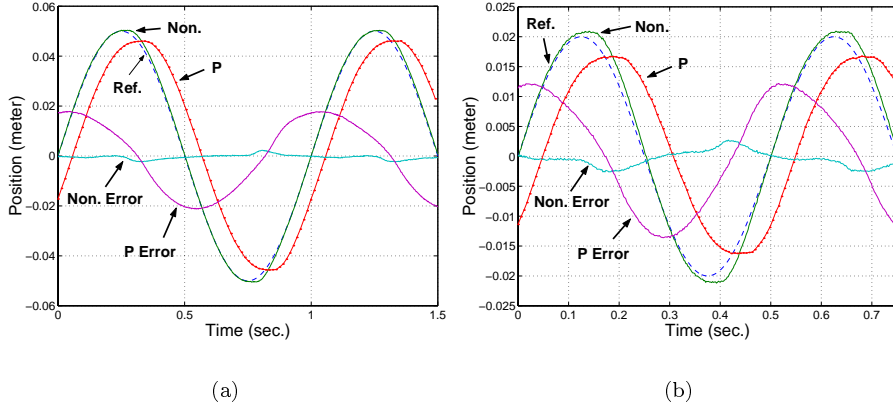


Figure 2. Position tracking along  $z$  coordinate (experiment). (a) 1HZ reference trajectory. (b) 2HZ reference trajectory.

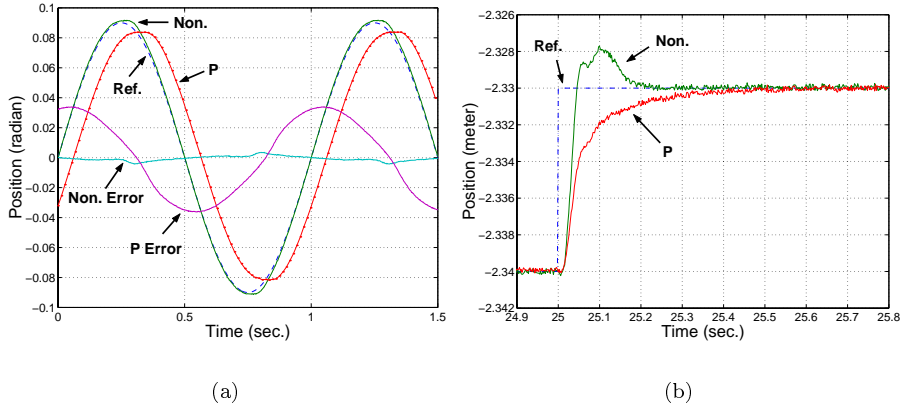


Figure 3. Experimental results. (a) 1HZ position tracking along  $\psi$  coordinate. (b) Step response along  $z$  coordinate.

Only the results of the experiments with adaptive controller/sliding observer are presented here while similar performance was observed for the other controller. Figure 2(a) shows the tracking behavior of the nonlinear controller compared with that of a well-tuned P controller in tracking the reference trajectory  $z_d = -2.34 + 0.05 \sin(2\pi t)$  meter (the bias is not shown). The maximum tracking errors are 4% and 43% for the nonlinear and P controller, respectively. The response of the system to a 2Hz reference trajectory was also examined and is presented in Figure 2(b). In this case  $z_d = -2.34 + 0.02 \sin(4\pi t)$  whereas the maximum tracking errors are 14% and 69%. Similar results were obtained in the other coordinates. For example, Figure 3(a) shows the tracking results along the  $\psi$  axis where  $\psi_d = 0.09 \sin(2\pi t)$  with 4% and 41% maximum tracking error for the nonlinear and P controller, respectively. In all of these cases the

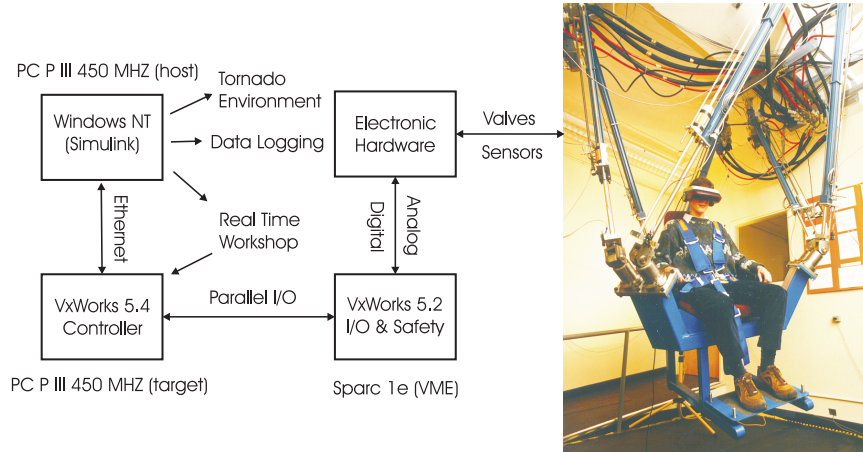


Figure 4. The experimental setup.

proposed adaptive nonlinear controller clearly outperforms the well-tuned P controller and exhibits excellent tracking performance.

During the experiments, the estimated parameters did not converge to fixed values, contrary to what was observed in simulations. Friction is an important factor which could introduce tracking errors and prevent the parameters from converging. The proposed controllers may be interpreted as cascade combinations of passivity-based position controllers and actuator force controllers. The very stiff dynamics of hydraulic actuators make the force (pressure) control loop sensitive to velocity estimation errors (or velocity measurement noise) and pressure measurement noise. This limits the level of the pressure feedback gains which may deteriorate the force tracking and subsequently parameter estimation, especially for the hydraulic parameters. Other factors such as unmodeled dynamics and insufficient excitation could also prevent parameter convergence. Moreover, it should be stressed that the parameter convergence is not even guaranteed in theory, so the experimental results do not contradict the theoretical arguments. The adaptation was found to be quite helpful in obtaining excellent tracking performance, which is the main goal of this research. In fact, it appears that parameters are adapted in way that reduces the tracking errors. The projection gains used in the adaptation laws proved effective in preventing the large parameter swings that can occur especially during start-up transients. The step response of the controller along the  $z$  axis is also compared with that of the P controller in Figure 3(b). As it can be seen, the nonlinear controller exhibits a much faster response with some overshoot.

## 6. Conclusions

This paper addressed the high performance position tracking control of hydraulic manipulators. Novel adaptive nonlinear controllers were proposed using the backstepping technique. Rigid body and hydraulic actuator models were incorporated in the design. These controllers feature novel adaptive and sliding

Table 1. The system parameters used in the simulations and experiments.

| Hydraulic Parameters  |                       |                            |                            |                            |
|-----------------------|-----------------------|----------------------------|----------------------------|----------------------------|
| Parameter             | $A$ (m <sup>2</sup> ) | $a$ (m <sup>2</sup> )      | $L$ (m)                    | $P_s$ (psi)                |
| Value                 | $1.14 \times 10^{-3}$ | $6.33 \times 10^{-4}$      | 1.37 m                     | 1500                       |
| Parameter             | $d$ (m)               | $c$                        | $\beta$ (Mpa)              | -                          |
| Value                 | $55.4 \times 10^{-6}$ | $1.5 \times 10^{-4}$       | 700                        | -                          |
| Rigid Body Parameters |                       |                            |                            |                            |
| Parameter             | $M_p$ (kg)            | $I_x$ (kg.m <sup>2</sup> ) | $I_y$ (kg.m <sup>2</sup> ) | $I_z$ (kg.m <sup>2</sup> ) |
| Value                 | 250                   | 45                         | 45                         | 43                         |

type observers to avoid acceleration feedback. The tracking errors were shown to converge to zero asymptotically (they are bounded by a gain-controlled bound in the presence of Coulomb friction) using Lyapunov analysis. Simulation and experimental data obtained using the UBC hydraulic Stewart platform are excellent and demonstrate the effectiveness of the proposed approach.

## References

- [1] Luh J, Walker M, Paul R 1980 Resolved acceleration control of mechanical manipulators. *IEEE Tran. Tran. Automat. Cont.* 25:468-474.
- [2] Berghuis H, Nijmeijer H 1993 A passivity approach to controller-observer design for robots. *IEEE Tran. Robot. Automat.* 9:740-754.
- [3] Ortega R, Spong M W 1989 Adaptive motion control of rigid robots: A tutorial. *Automatica* 25:877-888.
- [4] Spong M W 1992 On the robust control of robot manipulators. *IEEE Tran. Automat. Cont.* 37:1782-1786.
- [5] Su C -Y, Stepanenko Y 1998 Redesign of hybrid adaptive/robust motion control of rigid-link electrically-driven robot manipulator. *IEEE Tran. Robot. Automat.* 14:651-655.
- [6] Bu F and Yao B 2000 Observer-based coordinated adaptive robust control of robot manipulators driven by single-rod hydraulic actuators. In: *Proc. IEEE Int. Conf. Robot. Automat.*, pp. 3034-3039.
- [7] Sirouspour M R, Salcudean S E 2000 Nonlinear control of hydraulic robots. *conditionally accepted by IEEE Tran. Robot. Automat.*.
- [8] Sohl G A, Bobrow J E 1999 Experiments and simulations on the nonlinear control of a hydraulic servosystem. *IEEE Tran. Cont. Syst. Tech.* 7:238-247.
- [9] Sirouspour M R, Salcudean S E 2000 On the nonlinear control of hydraulic Servo-systems. In: *Proc. IEEE Int. Conf. Robot. Automat.*, pp. 1276-1282.
- [10] d'Annona-Novel B, Garnero M A, Abichou A 1994 Nonlinear control of a hydraulic robot using singular perturbations. In: *Proc. IEEE Int. Conf. Sys. Man and Cyber.*, pp. 1932-1937.
- [11] Edge K A, Gomes de Almeida F 1995 Decentralized adaptive control of a directly driven hydraulic manipulator part 1: theory. *Instn. Mech. Engrs.* 209:191-196.
- [12] Li D, Salcudean S E 1997 Modeling, simulation and control of a hydraulic Stewart platform. In: *Proc. IEEE Int. Conf. Robot. Automat.*, pp. 3360-3366.
- [13] Zhu W -H, De Schutter J 1999 Adaptive control of mixed rigid/flexible joint robot manipulators based on virtual decomposition. *IEEE Tran. Robot. Automat.*

15:310-317.

[14] Salcudean S E, Drexel P A, Ben-Dov D, et. al 1994 A six degree-of-freedom, hydraulic, one person motion simulator. In: *Proc. IEEE Int. Conf. Robot. Automat.*, pp. 859-864.

[15] Merritt H E 1967 *Hydraulic control systems*. Prentic-Hall Inc., New Jersey.

## Appendix A

The dynamics of a typical hydraulic actuator are presented in more detail in this Appendix. A three-way valve configuration is assumed to be used in the actuators as shown in Figure 5. For such a configuration, the control pressure dynamics are governed by [15]

$$\frac{V_t}{\beta} \dot{p}_c = q_l + c_l(p_s - p_c) - \dot{V}_t \quad (41)$$

where  $V_t$  is the trapped fluid volume in the control side,  $\beta$  is the effective bulk modulus,  $p_c$  is the control pressure acting on the control side,  $p_s$  is the supply pressure acting on the rod side,  $q_l$  is the load flow, and  $c_l$  is the coefficient of total leakage. The load flow,  $q_l$ , is a nonlinear function of the control pressure and the valve spool position and is given by

$$q_l = \begin{cases} c(u-d)\sqrt{p_c} & u < -d \\ c(u+d)\sqrt{p_s-p_c} + c(u-d)\sqrt{p_c} & -d \leq u \leq d \\ c(u+d)\sqrt{p_s-p_c} & u > d \end{cases} \quad (42)$$

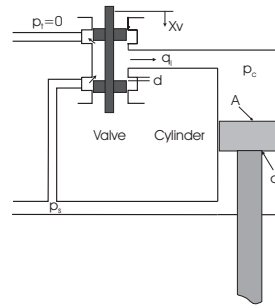


Figure 5. A typical three-way valve configuration.

and  $c = c_d w \sqrt{\frac{2}{\rho}}$  where  $c_d$  is the effective discharge coefficient,  $w$  is the port width of the valve,  $\rho$  is the density of the fluid,  $d$  is the valve underlap length and  $u$  is the valve spool position which is the control command. Note that the actuator output force is  $\tau = p_c A - p_s a$ . Therefore, using (41) and (42), the dynamics of  $i$ 'th hydraulic actuator can be written in the following form (assuming  $c_l \approx 0$ )

$$\dot{\tau}^i = -\frac{A\beta^i \dot{q}^i}{q^i - L} + \frac{\beta^i}{q^i - L} q_l^i(\tau^i, u^i) = f^i(q^i, \dot{q}^i) + g^i(q^i, \tau^i, u^i) \quad (43)$$

For a Stewart platform, there are six actuators driving the system. The actuator subsystem dynamics can be represented in matrix form as in (3).

Note that (43) can be rewritten in the following form which is suitable for adaptive control.

$$\dot{\tau}^i = \gamma_1^i f_0^i(q^i, \dot{q}^i) + \gamma_2^i g_0^i(q^i, \tau^i, u^i) \quad (44)$$

where  $\gamma^i = [\beta^i \quad \beta^i c^i]^T$ ,  $f_0^i = -\frac{A^i \dot{q}^i}{q^i - L^i}$ , and  $g_0^i = \frac{q_l^i}{c_i (q^i - L^i)}$  (does not depend on  $c_i$  see (42)). These equations can be written in matrix form as in (4).

## Appendix B

The Stewart platform is a parallel manipulator widely used in conventional motion simulators. The simplified rigid body dynamics of a typical Stewart platform are presented here.

In task-space coordinates, the dynamics of the platform are governed by (neglecting the leg dynamics):

$$D(q)\ddot{q} + C(q, \dot{q})\dot{q} + G = (JL)^T \tau \quad (45)$$

where  $q = [x \ y \ z \ \psi \ \theta \ \phi]^T$  is position of the platform with respect to a fixed frame and  $\phi$ ,  $\theta$  and  $\psi$  are the platform roll, pitch and yaw angles, respectively. Furthermore,  $J$  is the manipulator Jacobian matrix and  $L$  is a function of  $\theta$  and  $\phi$ .

$$L = \begin{bmatrix} I_{3 \times 3} & 0 \\ 0 & T \end{bmatrix}, \quad T = \begin{bmatrix} \cos(\theta) \cos(\phi) & -\sin(\phi) & 0 \\ \cos(\theta) \sin(\phi) & \cos(\phi) & 0 \\ -\sin(\theta) & 0 & 1 \end{bmatrix} \quad (46)$$

Finally,  $D(q)$ ,  $C(q, \dot{q})$  and  $G$  have the following forms:

$$\begin{aligned} D(q) &= \begin{bmatrix} M_p I_{3 \times 3} & 0 \\ 0 & T^T ({}^b I_p) T \end{bmatrix}, & C(q, \dot{q}) &= \begin{bmatrix} 0 & 0 \\ 0 & c_{22} \end{bmatrix} \\ c_{22} &= T^T \text{Skew}({}^b \omega_p) {}^b I_p T + T^T ({}^b I_p) \dot{T}, & G &= [0 \ 0 \ M_p g \ 0 \ 0 \ 0]^T \end{aligned} \quad (47)$$

where  $\omega$  is the angular velocity of the platform.

In the above equations,  ${}^b I_p$  is the platform inertia matrix with respect to the base frame and is given by

$${}^b I_p = R {}^p I_p R^T, \quad {}^p I_p = \begin{bmatrix} I_x & 0 & 0 \\ 0 & I_y & 0 \\ 0 & 0 & I_z \end{bmatrix} \quad (48)$$

and  $R$  is a rotation matrix representing the coordinates of the platform-attached base vectors in the base frame. Note that (45) is not exactly as (1). However, since  $J$  is a function of platform position and is known, the controllers can be easily modified to be used in this case. Moreover, the rigid body dynamics may be written in a linear-in-parameters form

$$D(q)\ddot{q} + C(q, \dot{q})\dot{q} + G = Y_{6 \times 4}(q, \dot{q}, \ddot{q})\theta, \quad (49)$$

where  $\theta = [M_p \ I_x \ I_y \ I_z]^T$  is a vector of kinematic and dynamic parameters. The detailed expressions of the elements of  $Y$  are long but fairly straightforward to derive and will not be presented here.